JOURNAL OF MOLECULAR SPECTROSCOPY 135, 197–206 (1989)

Heterodyne Frequency Measurements of $^{12}C^{16}O$ Laser Transitions

M. SCHNEIDER,[1] K. M. EVENSON, M. D. VANEK,
D. A. JENNINGS, AND J. S. WELLS

National Bureau of Standards, Boulder, Colorado 80303

AND

A. STAHN AND W. URBAN

Institut für Angewandte Physik, Universität Bonn, West Germany

This paper reports the first frequency measurements of a Lamb-dip-stabilized $^{12}C^{16}O$ laser. The laser was stabilized to the optogalvanic Lamb dip of the CO molecule excited in a low-pressure dc discharge. The region of study was for transitions with lower state vibrational quantum numbers ranging from $v'' = 6$ to $v'' = 16$. Supplementary Doppler limited measurements are also reported for the range $v'' = 16$ to $v'' = 34$. The frequencies were directly measured in a heterodyne experiment in which two saturation-stabilized CO_2 lasers were used as references. By fitting the transition frequencies to the Dunham expression, we have determined new coefficients which fit the new sub-Doppler data with over an order of magnitude more accuracy than previous coefficients.

INTRODUCTION

The energy levels of CO ($X^1\Sigma$) are well known, and the accuracy in the measurement of their spacings has been successively improved in the past few decades (see, for example, (*1–4*)). The most recent and by far most comprehensive wavelength measurements on CO have been performed by Guelachvili *et al.* in 1983 (*5*). He and his co-workers measured several thousand CO transitions from different emission and absorption sources. The wide range of measured rotational and vibrational transitions permits the determination of a set of 25 Dunham coefficients which accurately predict a large number of CO transition frequencies (including lasing transitions).

The strongest motivation for these measurements was the determination of the frequencies of the laser lines. These originate from highly excited vibrational states in CO (*6*). Since its discovery, the CO laser has served as a powerful spectroscopic source of coherent light in the mid infrared. Although the laser is not continuously tunable, the large number (several hundred) of laser lines is used for a variety of spectroscopic applications (see, for example, (*7–9*)). Most applications have made use of the lasing CO molecule by locking the laser to the top of its Doppler-broadened gain curve. The reproducibility of such a scheme of stabilization is typically several megahertz; however, by operating an unstabilized laser close to threshold, one can achieve a reproducibility

[1] Guest Scientist from Institut für Angewandte Physik, Universität Bonn, West Germany.

0022-2852/89 $3.00

of 1 MHz (*10*). Recent progress in the stabilization of the CO laser to CO itself (*11*) at the Institut für Angewandte Physik in Bonn has provided added impetus for the new frequency measurements reported here.

The data from the Fourier transform measurements made by Guelachvili *et al.* are Doppler-limited, and there are indications that laser frequencies predicted with Guelachvili's constants are systematically high in frequency by several megahertz (*12, 13*).

Prior to the measurements reported here, wavelength measurements and a few heterodyne frequency measurements have been made. Sokoloff mixed a CO laser with the CO_2 laser using a MIM diode and was able to determine one CO laser frequency (*14*). Eng, Kildal, and co-workers doubled the CO_2 laser in a nonlinear crystal and obtained a comb of reference frequencies in the CO laser region (*15, 16*); the lack of a high-order mixing technique restricted these measurements to a few accidental close coincidences between the CO laser and the doubled CO_2 laser. Furthermore, the CO_2 laser was not stabilized to a sub-Doppler feature.

During the past half-decade Wells and co-workers pursued accurate frequency measurements in the region 5 to 8 μm with a diode laser in which the CO laser was used as a transfer oscillator. Although the major emphasis was on the frequency measurements of OCS and N_2O (see, for example, Refs. (*17, 18*)) the CO laser frequencies were simultaneously measured in a synthesis scheme using two sub-Doppler-stabilized CO_2 lasers. While only those CO lines required for the primary objective were measured, a number of measurements have been accumulated. These also indicate that the values which are calculated with the molecular constants derived by Guelachvili are slightly high in frequency.

Pollock *et al.* (*19*) made accurate frequency measurements of the 2–0 overtone band; most of these measurements were made using CO Lamb dips. A color center laser was locked to the Lamb dips of CO while simultaneously being heterodyned with CO_2 laser references; the absolute uncertainty of these measurements was 100 kHz.

Freed reported Lamb dip stabilization of a low-pressure CO laser (*20*). Recently, we have shown that the CO laser can be stabilized by the optogalvanic detection technique to the saturation Lamb dip of the CO molecule itself (*11*). This permits a frequency lock with a stability and reproducibility of about 100 kHz, which is nearly two orders of magnitude more stable than previous Doppler-limited stabilization schemes. This increase in the stability makes it desirable to measure the frequency of this feature for each laser line, because direct frequency measurements can have orders of magnitude smaller uncertainties than the best wavelength measurements (which are limited by the physics of the measurement process: that is, by diffraction, phase shift, and index of refraction effects).

EXPERIMENTAL DETAILS

The CO laser is described in a number of earlier publications (see, for example, (*21, 22*)). The new scheme of optogalvanic Lamb dip detection and stabilization is described in detail in Ref. (*11*). In our present experiment the Lamb-dip-stabilized CO laser was built in a slightly different way. The present 2.7-m-long resonator uses a 200 line per millimeter grating and a 4-m radius coupling mirror with a reflectivity

of 95%. The gain cell and the low-pressure absorption cell are placed inside the laser resonator; both are sealed with NaCl Brewster windows. The cells are cooled by means of a methanol dry-ice cooling system. The saturation signal was detected optogalvanically in the low-pressure cell at a pressure of 173 Pa (1.3 Torr). The gas mixture contained Xe, CO, and N_2 in the relative ratios 3:2:2. The laser was stabilized using the third harmonic locking technique.

For our Doppler-limited measurements, we used a sealed CO laser, which was also dry-ice cooled. Some lines from higher vibrational states were also measured, and these were obtained from a liquid-nitrogen-cooled, flowing-gas CO laser.

Two CO_2 lasers were used as reference frequencies for our measurements. Both were locked to the CO_2 Lamb dip by means of the saturated fluorescence technique (*23*). The CO_2 frequencies are known (1σ) to 2 parts in 10^{10}, and the resettability is better than 1 part in 10^{10} (*24*). A W-Ni point contact diode was used as the nonlinear mixing device. The nonlinearity of the diode permits the generation of sums, differences, and harmonics of the frequencies of the impinging beams. The addition of microwave radiation of frequency, $\nu_{\mu w}$, to the diode permitted us to synthesize a frequency close to any CO laser transition at a frequency, ν_{CO}. This synthesized frequency, ν_s, was given by

$$\nu_s = m \cdot \nu'_{CO_2} + n \cdot \nu''_{CO_2} \pm \nu_{\mu w},$$

where m and n were either positive or negative integers, and the primed ν's are CO_2 laser frequencies. The difference between the synthesized frequency and the CO laser frequency, ν_{CO}, was a beat frequency, ν_B, which was extracted from the diode, amplified, and measured to determine the CO laser frequency. The frequency, ν_B, of the beat note was adjusted (by the choice of the microwave frequency) to fall within the 1.5-GHz range of our rf amplifier and rf spectrum analyzer. When the beat signal was displayed on a spectrum analyzer, a known frequency from a stable, separate synthesizer was simultaneously displayed and centered with the beat signal. This method permitted the reliable determination of the beat frequency. The CO laser frequency was

$$\nu_{CO} = \nu_s \pm \nu_B.$$

The major uncertainty in the measurements was due to the large modulation width of the CO laser (16 MHz peak to peak); this produced an uncertainty of ±300 kHz. The uncertainty for the Doppler-limited measurements is restricted by the reproducibility of the CO laser frequency setting; this was ±2.5 MHz for the sealed-off laser and ±3 MHz for the liquid-nitrogen-cooled, flowing-gas laser. Each measurement was repeated several times to confirm each frequency. Some lines did not yield reliable results because single line operation could not be easily maintained; these were not used for determining the new coefficients.

RESULTS

We measured 140 CO laser frequencies, of which 48 were sub-Doppler stabilized. We fitted these data to the well-known Dunham expression in which the energy levels of the CO molecule for given quantum numbers v and J are given by the expression

$$E(v, J) = \sum_{k,l} Y_{kl}(v + \tfrac{1}{2})^k (J(J+1))^l. \quad (1)$$

The set of 92 lines which could not be sub-Doppler stabilized was measured and also fitted in order to extend the fit and the predictability to other CO lines. In this fit we also took into account the sub-Doppler measurements from Pollock *et al.* (*19*) and the measurements from Hinz *et al.* (*25*).

A total number of 2357 CO transitions with vibrational quantum numbers up to $v'' = 41$ (data set number 1568 of "type B source" measurements from Ref. (*5*)) were also included in our fit. These FTS measurements had been taken by Guelachvili *et al.* using a laser-type discharge tube to excite the CO molecules into high vibrational–rotational states (for details see Ref. (*5*)). In order to take the known systematic shift of these frequencies into account, we attributed an uncertainty of 15 MHz to these frequencies.

Guelachvili *et al.* were able to determine a total of 25 Dunham coefficients due to the wide spectral range of their measurement. Absolute FTS wavelength measurements are subject to systematic shifts; however, they provide high accuracy in determining the wavelength differences of the recorded spectral lines. In order to make use of the high internal accuracy of the previous FTS measurements from Guelachvili, we attempted to take as many of his constants as fixed values into our fit. However, we had to float 19 constants of higher order to obtain observed − calculated values which did not show systematic dependence on vibrational or rotational quantum numbers. All 19 constants were very well determined in the new fit. Six other constants of higher order were fixed to the coefficients derived from Guelachvili *et al.* The estimated variance of the fit was 0.6. This is not close to unity due to the fact that the transition frequencies from Ref. (*5*) were included in the fit. The frequencies from Ref. (*5*) are better represented (especially in spectral regions where no heterodyne data were taken) by the new constants than by the uncertainty of 15 MHz which they were attributed. This uncertainty was chosen in order to take into account the systematic deviation between heterodyne and Fourier-transform data.

Table I shows the new set of Dunham coefficients. They reproduce our heterodyne measurements very well and simultaneously make use of the wide frequency spread of the measurement from Guelachvili *et al.* Numbers in parentheses represent the errors (1σ) of the corresponding constants. The matrix of the correlation coefficients has been inverted; its diagonal elements are also listed. Although the Dunham coefficients are often highly correlated, they are capable of describing the spectrum of CO over a broad range of rotational and vibrational quantum numbers. Due to the high correlation of the Dunham coefficients all constants are reported with 10 significant digits. This will avoid loss of precision in the calculated frequencies. Coefficients where no error is assigned are those which were taken from Ref. (*5*) and which were fixed in our fit.

Table II shows the list of measured frequencies. The assignment follows the convention where v'' and J'' correspond to the lower laser levels. The frequencies are calculated with the data set from Table I. The observed minus calculated (Obs. − Calc.) numbers show that our measurements are very well represented with the new constants. The numbers in parentheses in column 2 represent the uncertainties in the last sig-

TABLE I

Dunham Coefficients for $^{12}C^{16}O$ Laser Lines

Coef	Value [MHz]	Uncertainty [MHz]	Correlation[a]
Y_{01}	0.5789834412D+05	(0.784D-02)	1.07D2
Y_{02}	-0.1835195249D+00	(0.216D-04)	2.72D2
Y_{03}	0.1730174733D-06	(0.228D-07)	1.11D2
Y_{10}	0.6504933627D+08	(0.116D+01)	4.09D3
Y_{11}	-0.5247559337D+03	(0.928D-03)	1.41D2
Y_{12}	0.2718413289D-04	(0.192D-05)	2.22D2
Y_{13}	-0.4534252199D-08[b]		
Y_{20}	-0.3983542578D+06	(0.658D+00)	5.32D5
Y_{21}	0.1507565858D-01	(0.190D-03)	6.76D2
Y_{22}	-0.3793618583D-05	(0.214D-06)	2.06D2
Y_{23}	-0.4410831745D-10[b]		
Y_{30}	0.3108285993D+03	(0.139D+00)	1.79D7
Y_{31}	0.4646472836D-03	(0.911D-05)	1.74D3
Y_{32}	-0.1076462931D-06	(0.577D-08)	8.53D1
Y_{40}	0.2217510379D+01	(0.154D-01)	2.81D8
Y_{41}	0.4092398185D-04	(0.123D-06)	4.29D2
Y_{42}	0.4978153305D-08[b]		
Y_{50}	-0.3556930730D-02	(0.102D-02)	2.00D9
Y_{51}	-0.1747762292D-06[b]		
Y_{52}	-0.1413396166D-09[b]		
Y_{60}	0.3837288335D-03	(0.404D-04)	5.55D9
Y_{61}	-0.4299405019D-07[b]		
Y_{70}	-0.3260895808D-04	(0.954D-06)	5.49D9
Y_{80}	0.4589172485D-06	(0.123D-07)	1.61D9
Y_{90}	-0.2917514858D-08	(0.668D-10)	8.34D7

[a] correlation $\kappa_i = (\chi^{-1})_{ii}$, where χ is the matrix of correlation coefficients.
[b] coefficients taken as fixed numbers from Ref. 5

nificant digits (1σ) which we attribute to the respective measurement. In the fit, each data point was weighted with the inverse square of this uncertainty. The fitted constants reproduce the measured sub-Doppler data in Table II to an average Obs. − Calc. of −4 kHz with an rms deviation (1σ) of 150 kHz. The Doppler-limited data agree to an average Obs. − Calc. of −650 kHz with an rms deviation of 1250 kHz.

Figure 1 depicts the observed − calculated values from Table II (column 5) as a function of the corresponding laser frequency. The 13 laser frequencies for high vibrational levels from Ref. (*25*) are also represented in this figure. The error bars indicate the uncertainties we attributed to the measurements due to read-out uncertainty and uncertainty in the resettability of the laser frequency. For each line measured the difference between the calculated frequency using the "new" constants and the frequency using the constants from (*5*) are also shown. In the high-frequency part of the laser spectrum, a systematic deviation is evident: the FTS numbers are higher than ours by almost 10 MHz. This shift for higher frequencies was already indicated by the heterodyne measurements of Pollock *et al.* (*19*), Brown *et al.* (*12*) and Jennings *et al.* (*13*). From Fig. 1, it is obvious that the new constants predict CO laser frequencies much more accurately in the spectral region where our heterodyne frequency measurements were made.

TABLE II

Heterodyne Frequency Measurements on $^{12}C^{16}O$

CO $P(J'')_{v''}$	Observed Frequency [MHz]	Calculated Frequency [MHz]	[cm^{-1}]	Obs.-Calc. [MHz]
$P(14)_6$	57902072.86(250)	57902071.45	1931.40521	1.41
$P(15)_6$	57778875.40(250)	57778873.59	1927.29577	1.81
$P(17)_6$	57529533.23(30)	57529533.43	1918.97868	-0.20
$P(18)_6$	57403399.62(30)	57403399.88	1914.77131	-0.26
$P(19)_6$	57276296.31(30)	57276296.51	1910.53160	-0.20
$P(13)_7$	57256686.14(30)	57256686.40	1909.87748	-0.26
$P(14)_7$	57135526.56(30)	57135526.61	1905.83602	-0.05
$P(15)_7$	57013379.50(30)	57013379.64	1901.76164	-0.14
$P(16)_7$	56890249.71(30)	56890249.86	1897.65447	-0.15
$P(17)_7$	56766141.66(30)	56766141.66	1893.51467	0.00
$P(12)_8$	56610485.07(30)	56610484.72	1888.32251	0.35
$P(13)_8$	56491367.10(30)	56491367.15	1884.34918	-0.05
$P(14)_8$	56371258.20(30)	56371258.17	1880.34277	0.03
$P(16)_8$	56128083.52(30)	56128083.51	1872.23134	0.01
$P(18)_8$	55880995.98(30)	55880995.73	1863.98938	0.25
$P(13)_9$	55728370.10(30)	55728370.28	1858.89834	-0.18
$P(14)_9$	55609312.12(30)	55609312.16	1854.92699	-0.04
$P(15)_9$	55489267.23(30)	55489267.18	1850.92272	0.05
$P(16)_9$	55368239.70(30)	55368239.72	1846.88568	-0.02
$P(17)_9$	55246234.17(30)	55246234.15	1842.81601	0.02
$P(13)_{10}$	54967739.05(30)	54967739.16	1833.52642	-0.11
$P(14)_{10}$	54849731.99(30)	54849731.91	1829.59012	0.08
$P(17)_{10}$	54489807.60(30)	54489807.62	1817.58434	-0.02
$P(12)_{11}$	54325479.05(30)	54325479.46	1812.10294	-0.41
$P(13)_{11}$	54209513.77(30)	54209513.88	1808.23474	-0.11
$P(14)_{11}$	54092557.48(30)	54092557.47	1804.33350	0.01
$P(15)_{11}$	53974614.45(30)	53974614.59	1800.39935	-0.14
$P(18)_{11}$	53614910.99(30)	53614910.84	1788.40092	0.15
$P(12)_{12}$	53568645.67(30)	53568645.64	1786.85768	0.03
$P(13)_{12}$	53453730.55(30)	53453730.62	1783.02453	-0.07
$P(14)_{12}$	53337824.95(30)	53337824.98	1779.15833	-0.03
$P(15)_{12}$	53220932.92(30)	53220933.08	1775.25924	-0.16
$P(17)_{12}$	52984207.97(30)	52984208.00	1767.36294	-0.03
$P(18)_{12}$	52864383.72(30)	52864383.55	1763.36603	0.17
$P(13)_{13}$	52700420.97(30)	52700421.00	1757.89682	-0.03
$P(14)_{13}$	52585565.95(30)	52585566.00	1754.06567	-0.05
$P(15)_{13}$	52469724.96(30)	52469724.97	1750.20163	-0.01
$P(16)_{13}$	52352902.38(30)	52352902.28	1746.30485	0.10
$P(17)_{13}$	52235102.44(30)	52235102.28	1742.37546	0.16
$P(18)_{13}$	52116329.34(30)	52116329.35	1738.41362	-0.01
$P(12)_{14}$	52062425.74(30)	52062425.75	1736.61559	-0.01
$P(13)_{14}$	51949611.44(30)	51949611.40	1732.85251	0.04
$P(14)_{14}$	51835806.97(30)	51835806.86	1729.05640	0.11
$P(15)_{14}$	51721016.57(30)	51721016.52	1725.22741	0.05
$P(16)_{14}$	51605244.67(30)	51605244.74	1721.36568	-0.07
$P(18)_{14}$	51370774.42(30)	51370774.29	1713.54458	0.13
$P(13)_{15}$	51201322.54(30)	51201322.29	1707.89227	0.25
$P(14)_{15}$	51088568.12(30)	51088567.97	1704.13119	0.15
$P(12)_{16}$	50566282.51(30)	50566282.22	1686.70962	0.29
$P(20)_{15}$	50391497.25(250)	50391497.35	1680.87942	-0.10
$P(14)_{16}$	50343863.29(30)	50343863.11	1679.29051	0.18
$P(21)_{15}$	50271937.30(250)	50271935.43	1676.89127	1.87
$P(16)_{15}$	50117500.62(250)	50117502.49	1671.73994	-1.87
$P(17)_{16}$	50002854.62(250)	50002855.03	1667.91571	-0.41
$P(12)_{17}$	49822018.33(250)	49822019.11	1661.88367	-0.78
$P(19)_{16}$	49770648.00(250)	49770647.58	1660.17010	0.42
$P(13)_{17}$	49712353.19(250)	49712353.70	1658.22563	-0.51
$P(20)_{16}$	49653097.19(250)	49653096.27	1656.24901	0.92
$P(15)_{17}$	49490059.16(250)	49490058.64	1650.81066	0.52
$P(16)_{17}$	49377438.31(250)	49377437.71	1647.05403	0.60
$P(18)_{17}$	49149270.24(250)	49149270.83	1639.44321	-0.59
$P(12)_{18}$	49080292.68(250)	49080295.95	1637.14245	-3.27
$P(13)_{18}$	48971679.05(250)	48971679.36	1633.51939	-0.31
$P(20)_{17}$	48917233.44(250)	48917232.94	1631.70325	0.50
$P(12)_{18}$	49080292.68(250)	49080295.95	1637.14245	-3.27
$P(13)_{18}$	48971679.05(250)	48971679.36	1633.51939	-0.31
$P(20)_{17}$	48917233.44(250)	48917232.94	1631.70325	0.50
$P(14)_{18}$	48862073.00(250)	48862073.40	1629.86333	-0.40
$P(8)_{19}$	48761396.61(250)	48761396.24	1626.50510	0.37
$P(15)_{18}$	48751482.18(250)	48751482.44	1626.17441	-0.26
$P(10)_{19}$	48553253.28(250)	48553254.18	1619.56223	-0.90
$P(18)_{18}$	48413842.55(250)	48413843.16	1614.91198	-0.61
$P(12)_{19}$	48341101.26(250)	48341102.68	1612.48562	-1.42
$P(19)_{18}$	48299355.39(250)	48299355.76	1611.09309	-0.37
$P(13)_{19}$	48233534.00(250)	48233534.34	1608.89752	-0.34

The estimated uncertainty in the last digits are given in parentheses.
The last 13 measurements are taken from reference 25.

TABLE II—*Continued*

CO $P(J'')_{v''}$	Observed Frequency [MHz]	Calculated Frequency [MHz]	[cm^{-1}]	Obs.-Calc. [MHz]
$P(20)_{18}$	48183905.31(250)	48183905.12	1607.24207	0.19
$P(8)_{20}$	48020524.65(250)	48020523.97	1601.79226	0.68
$P(15)_{19}$	48015432.77(250)	48015434.36	1601.62249	-1.59
$P(9)_{20}$	47918004.05(250)	47918003.52	1598.37255	0.53
$P(16)_{20}$	47904910.43(250)	47904911.44	1597.93584	-1.01
$P(10)_{19}$	47814477.00(250)	47814476.43	1594.91926	0.57
$P(17)_{20}$	47793411.89(250)	47793412.38	1594.21664	-0.49
$P(18)_{19}$	47680941.66(250)	47680941.53	1590.46501	0.13
$P(12)_{20}$	47604420.66(250)	47604419.83	1587.91252	0.83
$P(19)_{20}$	47567502.24(250)	47567503.23	1586.68112	-0.99
$P(13)_{19}$	47497899.11(250)	47497899.10	1584.35937	0.01
$P(20)_{19}$	47453101.42(250)	47453101.81	1582.86510	-0.39
$P(9)_{21}$	47180662.08(250)	47180661.20	1573.77746	0.88
$P(15)_{21}$	46550832.24(250)	46550833.35	1552.76866	-1.11
$P(8)_{22}$	46546191.04(250)	46546189.08	1552.61374	1.96
$P(9)_{22}$	46445760.86(250)	46445761.44	1549.26384	-0.58
$P(16)_{22}$	46442404.90(300)	46442405.32	1549.15189	-0.42
$P(10)_{21}$	46344326.60(300)	46344327.16	1545.88036	-0.56
$P(19)_{21}$	46111281.28(250)	46111282.57	1538.10682	-1.29
$P(13)_{22}$	46034028.17(250)	46034028.42	1535.52990	-0.25
$P(14)_{22}$	45928609.70(300)	45928611.46	1532.01357	-1.76
$P(8)_{23}$	45812635.10(300)	45812634.61	1528.14500	0.49
$P(9)_{23}$	45713253.76(250)	45713252.48	1524.82997	1.28
$P(12)_{23}$	45409085.80(300)	45409083.18	1514.68397	2.62
$P(19)_{22}$	45386840.32(250)	45386842.56	1513.94211	-2.24
$P(15)_{23}$	45095969.91(250)	45095971.57	1504.23970	-1.66
$P(9)_{24}$	44983071.00(300)	44983070.30	1500.47371	0.70
$P(10)_{24}$	44883726.30(300)	44883726.06	1497.15995	0.24
$P(11)_{24}$	44783379.90(300)	44783379.27	1493.81274	0.63
$P(12)_{24}$	44682033.90(300)	44682034.31	1490.43223	-0.41
$P(14)_{24}$	44476365.20(300)	44476367.39	1483.57192	-2.19
$P(15)_{24}$	44372051.80(300)	44372054.15	1480.09241	-2.35
$P(10)_{25}$	44156837.10(300)	44156837.42	1472.91355	-0.32
$P(18)_{24}$	44053245.44(250)	44053247.59	1469.45817	-2.15
$P(12)_{25}$	43957232.40(300)	43957232.37	1466.25544	0.03
$P(13)_{25}$	43855934.80(300)	43855936.48	1462.87658	-1.68
$P(20)_{24}$	43835859.82(250)	43835864.14	1462.20704	-4.32
$P(14)_{25}$	43753650.59(250)	43753650.86	1459.46470	-0.27
$P(11)_{26}$	43333843.60(300)	43333845.95	1445.46151	-2.35
$P(15)_{26}$	42930857.00(300)	42930857.15	1432.01925	-0.15
$P(8)_{27}$	42900849.00(300)	42900850.73	1431.01835	-1.73
$P(12)_{27}$	42513988.00(300)	42513990.17	1418.11407	-2.17
$P(16)_{27}$	42111205.00(300)	42111206.50	1404.67865	-1.50
$P(9)_{28}$	42083851.80(300)	42083855.48	1403.76632	-3.68
$P(10)_{28}$	41988681.50(300)	41988681.24	1400.59165	0.26
$P(12)_{28}$	41795321.60(300)	41795322.93	1394.14191	-1.33
$P(13)_{28}$	41697146.00(300)	41697147.64	1390.86713	-1.64
$P(15)_{28}$	41497824.80(300)	41497826.58	1384.21850	-1.78
$P(9)_{29}$	41363861.10(300)	41363861.99	1379.74992	-0.89
$P(10)_{29}$	41269726.80(300)	41269727.89	1376.60994	-1.09
$P(13)_{29}$	40981307.00(300)	40981308.77	1366.98932	-1.77
$P(7)_{30}$	40828659.50(300)	40828659.90	1361.89750	-0.40
$P(15)_{29}$	40784058.20(300)	40784059.07	1360.40978	-0.87
$P(12)_{30}$	40363206.30(300)	40363207.10	1346.37167	-0.80
$P(14)_{30}$	40170007.70(300)	40170007.99	1339.92724	-0.29
$P(8)_{31}$	40019664.80(300)	40019665.60	1334.91235	-0.80
$P(9)_{31}$	39928620.40(300)	39928621.58	1331.87545	-1.18
$P(10)_{31}$	39836563.00(300)	39836564.73	1328.80477	-1.73
$P(14)_{31}$	39458296.30(300)	39458296.97	1316.18711	-0.67
$P(16)_{31}$	39263198.20(300)	39263199.95	1309.67938	-1.75
$P(11)_{31}$	39029957.20(300)	39029958.95	1301.89929	-1.75
$P(13)_{32}$	38842887.60(300)	38842886.10	1295.65922	1.50
$P(8)_{33}$	38587420.90(300)	38587423.16	1287.13789	-2.26
$P(9)_{33}$	38498453.10(300)	38498456.12	1284.17027	-3.02
$P(10)_{33}$	38408472.30(300)	38408472.43	1281.16874	-0.13
$P(12)_{33}$	38225471.60(300)	38225472.70	1275.06452	-1.10
$P(8)_{34}$	37872657.90(300)	37872657.92	1263.29589	-0.02
$P(10)_{34}$	37695777.70(300)	37695779.76	1257.39587	-2.06

We have calculated the frequencies of a CO laser spectrum over a wider range (with quantum numbers ranging from $v'' = 2$ to $v'' = 37$ and $J'' = 3$ to $J'' = 25$, respectively). Figure 2 shows the differences between these two calculated spectra; one was calculated

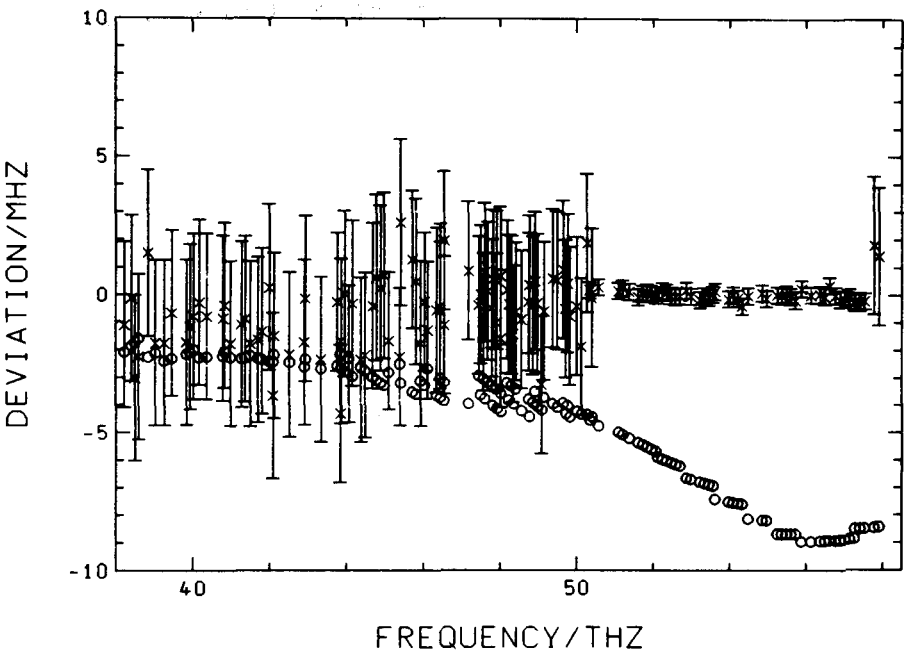

FIG. 1. Differences between our observed and our calculated values from Table II (column 5) depicted (×) as a function of the corresponding laser frequency. The error bars indicate the uncertainty we attributed to our measurements. The differences between our calculated frequencies (column 3 in Table II) and the frequencies calculated with the Dunham coefficients from Ref. (*5*) are also shown (○) for the lines which were measured. The latter are higher in frequency than those from this present work by as much as 10 MHz. The data points at 40 THz and below are taken from Ref. (*25*).

with our new set of Dunham coefficients from Table I, and the other was calculated with the Dunham coefficients derived by Guelachvili.

In the frequency range from 40 to 58 THz a smooth curve results as is shown in Fig. 2; i.e., both sets predict the differences quite accurately; however, the several megahertz difference in the absolute frequencies previously mentioned is obvious in the figure. Below 40 and above 58 THz, a significant spread becomes obvious; the absolute frequency of a CO laser transition is better represented by the new Dunham coefficients, but the difference between two CO transitions in the same band could be better represented by Guelachvili's Dunham coefficients.

SUMMARY

Frequency measurements using a Lamb-dip-stabilized CO laser permitted much more accurate measurements of CO laser frequencies than have been obtained previously. These frequencies of the sub-Doppler feature were measured for the first time in heterodyne experiments. Additional new Doppler-limited measurements have also been made. The new frequency values differ from previous FTS measurements by 1

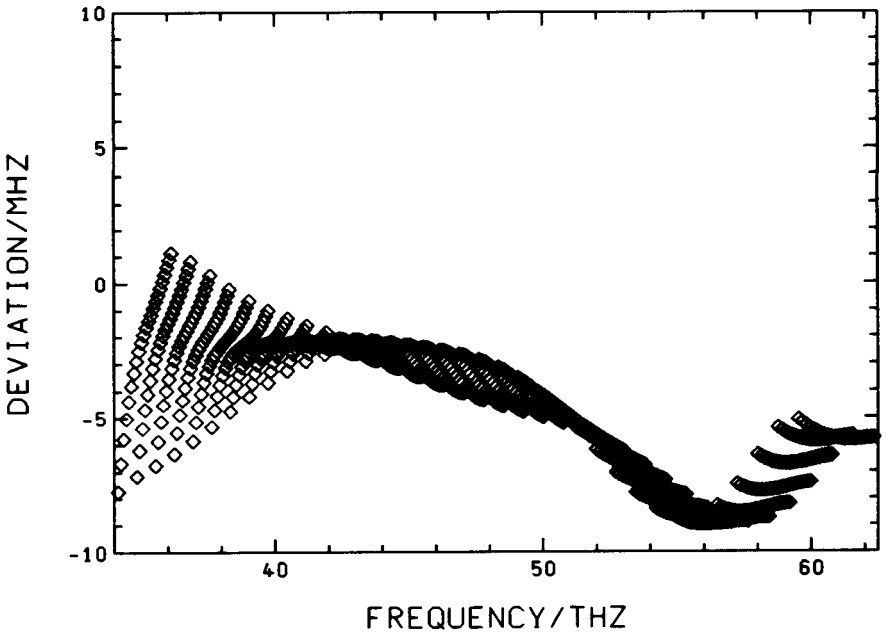

FIG. 2. Frequency difference between two CO laser spectra based on two different sets of Dunham coefficients. One spectrum was calculated using the constants from Table I, and the other was calculated using the constants from Ref. (*5*). The latter is higher in frequency than the spectrum based on the present heterodyne experiment. The spectra were calculated for all quantum numbers v'' and J'' with $2 \leq v'' \leq 37$ and $3 \leq J'' \leq 25$.

to 10 MHz. In order to be able to better describe the spectrum of CO, the new frequencies were fit to the Dunham formula. Nineteen coefficients were redetermined while six higher-order coefficients were fixed to the values in Ref. (*5*). This new set of Dunham coefficients predicts laser frequencies between 50 and 58 THz with an rms deviation (1σ) of 150 kHz. The set predicts the frequencies from 38 to 50 THz to ± 2 MHz, and to ± 5 MHz between 34 and 40, and from 58 to 62 THz. Since CO transition frequencies from Refs. (*5, 19, 25*) were included in our fit, the set of new constants cover a broader spectral range of transitions than our measurements. For CO transitions well outside the region where the laser is operating, the frequencies from Guelachvili *et al.* probably provide better frequency differences than ours due to the wider range of their measurements. However, the new constants yield more accurate absolute frequencies of the CO transitions on which the laser oscillates, especially those in which the laser lines can be stabilized to the CO Lamb dip. Tables of frequency of CO laser transitions have been calculated (*26*)[2] using the constants from Table I which have been derived in this work. These tables are available as NIST (formerly NBS) Special Publication No. 1321 or on request from the authors.

[2] A limited number of copies are on deposit in the Editorial Office. Please contact K.M.E. at NIST first if you are interested in these tables.

ACKNOWLEDGMENTS

We are grateful to G. Guelachvili for providing the magnetic tape with the set of CO transition frequencies from the Fourier-transform measurements. We thank Th. Nelis and A. Hinz for many discussions and comments. M.S. thanks his colleagues in the Time and Frequency Division at the NBS for their warm hospitality and help during the collaboration. The collaboration has been partly supported by a grant from the Deutscher Akademischer Austauschdienst. K.M.E. also thanks the Alexander von Humboldt Foundation for providing the funding for his stay at the University of Bonn where this work was initiated. Portions of this work were facilitated by NASA Grant No. W-14,587.

RECEIVED: December 7, 1988

REFERENCES

1. A. W. MANTZ, E. R. NICHOLS, B. D. ALPERT, AND K. NARAHARI RAO, *J. Mol. Spectrosc.* **35,** 325–318 (1970).
2. W. B. ROH AND K. NARAHARI RAO, *J. Mol. Spectrosc.* **49,** 317–321 (1974).
3. R. M. DALE, M. HERMAN, J. W. C. JOHNS, A. R. W. MCKELLAR, S. NAGLER, AND I. K. M. STRATHY, *Canad. J. Phys.* **57,** 677–686 (1979).
4. G. GUELACHVILI, *J. Mol. Spectrosc.* **75,** 251–269 (1979).
5. G. GUELACHVILI, D. DE VILLENEUVE, R. FARRENQ, W. URBAN, AND J. VERGES, *J. Mol. Spectrosc.* **98,** 64–79 (1983).
6. C. K. N. PATEL, *Phys. Rev.* **141,** 71–83 (1966).
7. W. H. WEBER, P. D. MAKER, J. W. C. JOHNS, AND E. WEINBERGER, *J. Mol. Spectrosc.* **121,** 243–260 (1987).
8. W. ROHRBECK, A. HINZ, P. NELLE, M. A. GONDAL, AND W. URBAN, *Appl. Phys. B* **31,** 139–144 (1983).
9. S.-C. HSU, R. H. SCHWENDEMAN, AND G. MAGERL, *IEEE J. Quantum Electron.,* **24,** 2294–2301 (1988).
10. L. S. MASUKIDI, J.-G. LAHAYE, B. COVELIERS, AND A. FAYT, *J. Opt. Soc. Amer. B* **4,** 1177 (1987).
11. M. SCHNEIDER, A. HINZ, A. GROH, K. M. EVENSON, AND W. URBAN, *Appl. Phys. B* **44,** 241–245 (1987).
12. L. R. BROWN AND R. A. TOTH, *J. Opt. Soc. Amer. B* **2,** 842–856 (1985).
13. D. E. JENNINGS AND J. W. BRAULT, *J. Mol. Spectrosc.* **102,** 265–272 (1983).
14. D. R. SOKOLOFF, A. SANCHEZ, R. M. OSGOOD, AND A. JAVAN, *Appl. Phys. Lett.* **17,** 257–259 (1970).
15. R. S. ENG, H. KILDAL, J. C. MIKKELSEN, AND D. L. SPEARS, *Appl. Phys. Lett.* **24,** 231–233 (1974).
16. H. KILDAL, R. S. ENG, AND A. H. M. ROSS, *J. Mol. Spectrosc.* **53,** 479–488 (1974).
17. J. S. WELLS, F. R. PETERSEN, AND A. G. MAKI, *J. Mol. Spectrosc.* **98,** 404–412 (1983).
18. J. S. WELLS, A. HINZ, AND A. G. MAKI, *J. Mol. Spectrosc.* **114,** 84–96 (1985).
19. C. R. POLLOCK, F. R. PETERSEN, D. A. JENNINGS, J. S. WELLS, AND A. G. MAKI, *J. Mol. Spectrosc.* **99,** 357–368 (1983).
20. C. FREED AND H. A. HAUS, *IEEE J. of Quant. Electron.* **QE-9,** 219–226 (1973).
21. C. FREED, *Appl. Phys. Lett.* **18,** 458–461 (1971).
22. T. X. LIN, W. ROHRBECK, AND W. URBAN, *Appl. Phys. B* **26,** 73–76 (1981).
23. C. FREED AND A. JAVAN, *Appl. Phys. Lett.* **17,** 53–56 (1970).
24. F. R. PETERSEN, E. C. BEATY, AND C. R. POLLOCK, *J. Mol. Spectrosc.* **102,** 112–122 (1983).
25. A. HINZ, J. S. WELLS, AND A. G. MAKI, *Z. Phys. D.* **5,** 351–358 (1987).
26. M. SCHNEIDER, K. M. EVENSON, M. D. VANEK, D. A. JENNINGS, J. S. WELLS, A. STAHN, AND W. URBAN, NBS Technical Note No. 1321 (1988).